HHS Public Access

Author manuscript

AJR Am J Roentgenol. Author manuscript; available in PMC 2016 October 01.

Published in final edited form as:

AJR Am J Roentgenol. 2015 October ; 205(4): 899–904. doi:10.2214/AJR.14.13804.

Detection of Internal Mammary Adenopathy in Patients With Breast Cancer by PET/CT and MRI

Maxine S. Jochelson[1], **Lizza Lebron**, **Stefanie S. Jacobs**, **Junting Zheng**, **Chaya S. Moskowitz**, **Simon N. Powell**, **Virgilio Sacchini**, **Gary A. Ulaner**, **Elizabeth A. Morris**, and **D. David Dershaw**

Memorial Sloan Kettering Cancer Center, 1275 York Ave, New York, NY 10065

Abstract

OBJECTIVE—The purpose of this study was to assess the prevalence of internal mammary node (IMN) adenopathy in patients with breast cancer and compare breast MRI and PET/CT for detection of IMN adenopathy.

MATERIALS AND METHODS—This retrospective study included 90 women who underwent MRI and PET/CT before neoadjuvant chemotherapy for clinical stage IIA through IIIA disease. MRI and PET/CT examinations were read independently by two readers trained in breast imaging and nuclear medicine. All patients underwent follow-up MRI at the end of chemotherapy, and 10 with hypermetabolic IMNs underwent follow-up PET/CT. Histology was not obtained. Women were considered to have IMN adenopathy when nodes seen on MRI or having standardized uptake value (SUV) greater than mediastinal blood pool decreased in either size or SUV (or both) after treatment. Features including lymphovascular invasion, tumor quadrant(s), and axillary adenopathy were compared between presence and absence of IMN adenopathy using Fisher's exact test. Prevalence was determined on the basis of the percentage of patients with IMN adenopathy by either modality. The McNemar test compared the prevalence of IMN adenopathy on MRI to its prevalence on PET/CT.

RESULTS—Prevalence of IMN adenopathy was 16% (14/90) by MRI and 14% (13/90) by PET/CT ($p = 0.317$). After chemotherapy, IMN adenopathy resolved in 12 of 14 patients (86%). In two patients with poor responses in primary tumors, IMN adenopathy persisted, and both patients developed metastatic disease within 6 months. At 3 years, survival was significantly worse in patients with IMN adenopathy than in those without (85.7% vs 53.3%, respectively; $p = 0.009$).

CONCLUSION—In women with advanced breast cancer receiving neoadjuvant chemotherapy, prevalence of IMN adenopathy was 16%, equally detected by breast MRI and PET/CT. Identification of IMN adenopathy may affect treatment and provides prognostic information.

Keywords

breast cancer; breast MRI; internal mammary nodes; neoadjuvant chemotherapy; PET/CT

[1]Address correspondence to M. S. Jochelson (jochelsm@mskcc.org).

In women with newly diagnosed breast cancer, the discovery of internal mammary node (IMN) metastases will upstage a patient with clinical stage I or II disease to stage III. IMN adenopathy is a known poor prognostic factor with demonstrable higher rates of distant disease and worse survival [1–3]. Although there is controversy surrounding this issue, recent data suggest that treatment with systemic chemotherapy and radiation therapy may improve outcome in patients with IMN adenopathy [4, 5]. However, radiation therapy to the internal mammary chain may also increase cardiac toxicity and should not be used unnecessarily. Therefore, accurate identification of IMN adenopathy is an important factor in the initial staging of women with breast cancer.

The prevalence of IMN adenopathy increases with increasing tumor size, presence of axillary adenopathy, lymphovascular invasion (LVI), decreasing patient age, and inner quadrant tumors [4, 6, 7]. Patients with larger breast tumors—who are at higher risk of extraaxillary adenopathy, as well as distant metastases— often undergo both breast MRI and PET/CT at initial presentation. PET/CT has been shown to be more accurate in the detection of IMN adenopathy than CT alone [8–10]. Breast MRI also detects IMN adenopathy, but little has been written about its ability to do so in this setting. The purpose of this study is to determine the prevalence of IMN adenopathy in patients with untreated breast cancer before receiving neoadjuvant chemotherapy and to compare breast MRI to PET/CT for detection of IMN adenopathy.

Materials and Methods

Patients

This was a retrospective institutional review board–approved, HIPAA-compliant study of 90 consecutive women 25–72 years old who underwent imaging with both PET/CT and breast MRI before receiving neoadjuvant chemotherapy for clinical stages IIA through IIIA (T2–3N0 or T1–3N1–3) disease from 2009 to 2012. Clinical histories and images were reviewed.

Histologic diagnosis of the primary tumor was made by image-guided percutaneous core biopsy in all cases. Histologic diagnosis of axillary adenopathy was made by fine-needle aspiration in 59 of 90 patients including 11 of 14 patients with IMN adenopathy. Ten of 90 patients underwent core needle biopsies of axillary nodes including one of 14 patients with IMN adenopathy. Twenty of 90 patients had no axillary sampling, one of whom was a patient with IMN adenopathy.

The time interval between tissue sampling of the primary tumor or axillary nodes (or both) and imaging ranged from 0 to 86 days, with three patients undergoing imaging before biopsies. The mean time interval was 16.3 days, and the median was 14 days. The time between biopsy and imaging in the patients with IMN adenopathy ranged from 0 to 33 days, with a mean of 14.6 and a median of 12 days.

Eighty-five patients had invasive ductal carcinoma, two had invasive mammary carcinoma, and three had invasive lobular carcinoma. Six women had inflammatory breast carcinoma. Baseline tumor size was assessed by breast MRI. Forty patients had *ERBB2* (formerly *HER2* or *HER2/neu*)–positive disease, 15 patients had estrogen receptor or progesterone

receptor–positive *ERBB2*-negative disease, and 35 patients had triple-negative disease (i.e., negative for all three of the aforementioned markers). Chemotherapy regimens administered were dependent on marker status. Presence of IMN adenopathy was correlated with tumor quadrant, axillary adenopathy, and LVI.

Imaging

Thirty-six of the initial breast MRI examinations and 30 of the initial PET/CT examinations were performed at outside institutions and were considered to be of adequate quality for patient care. Any other, poor-quality examinations were repeated at our institution, and the repeat examinations were used for the purpose of this study. The time interval between the initial MRI and PET/CT scan was 0–33 days (median, 5 days). All follow-up examinations were performed at our institution.

Fluorine-18-FDG PET/CT—Patients fasted for at least 6 hours before ^{18}F-FDG injection. Each patient was injected IV with 12–15mCi (444–555 MBq) of ^{18}F-FDG when plasma glucose level was less than 200 mg/dL, after which there was a 60- to 90-minute tracer uptake period. Scans were acquired supine from the base of the skull to the mid thigh. In most cases, low-dose CT scans with oral contrast material were obtained. FOV was 70 cm for PET and 50 cm for CT. In-plane resolution was 5.4 mm. Slice thickness for CT was 3.75 mm. Tube current–exposure time product ranged from 40 to 100 mAs depending on weight, and tube voltage was 140 kVp. Attenuation-corrected images were reviewed on a PACS workstation (AW Suite, GE Healthcare).

MRI—Pretreatment MRI examinations were often performed at outside institutions and therefore used a variety of techniques. MRI at our institution, which was the posttreatment follow-up study for all patients, was performed with the patient prone in a dedicated surface breast coil on a 1.5- or 3.0-T commercially available system. Both breasts were imaged simultaneously using Vibrant (GE Healthcare). The standard examination included a localizing sequence followed by a sagittal T2 fast spin-echo sequence using fat suppression with TR/TE = 3000/15. A T1 non–fat-suppressed sequence was performed with TR/TE = 4.8/2.1. A sagittal T1-weighted 3D fat-suppressed fast spoiled gradient-echo sequence was performed before and three times after a rapid IV bolus injection of 0.1 mmol/L of gadopentetate dimeglumine (Magnevist, Bayer HealthCare) per kilogram of body weight followed by a saline bolus, with the following parameters: TR/TE = 11.1/2.1 (in phase), section thickness of 0.3 cm with no gap, and a minimum matrix of 256 × 256. Unenhanced images were subtracted from the contrast-enhanced images on a pixel-by-pixel basis, producing three contrast-enhanced subtraction sequences. Maximum-intensity-projection images were created using the first contrast-enhanced sequence and the first contrast-enhanced subtraction sequence. Delayed axial images were acquired with special fat suppression and TR/TE = 5.5/2.1.

Image Interpretation

Breast MRI and PET/CT examinations were read independently by two readers with 3 and 12 years' experience in breast imaging and nuclear medicine. Initially each reader interpreted the MRI followed by the PET/CT study on each patient. Several weeks later they

reread the PET/CT studies independently to ensure that the PET/CT findings were not influenced by the MRI findings. On the MRI studies, reviewers evaluated the contrast-enhanced axial and sagittal images when available on both in-house and outside examinations. The readers evaluated all the intercostal spaces. IMNs were differentiated from internal mammary vessels by scrolling through the images in both the sagittal and axial planes. IMNs were measured and recorded on both MRI and the CT portion of the PET/CT examinations. Patients were considered to have IMN adenopathy when IMNs were seen discretely on MRI regardless of size or when standardized uptake value (SUV) of a visualized IMN was greater than mediastinal blood pool on PET/CT (Fig. 1). In five cases in which the original two readers did not agree on the evaluation of the internal mammary nodes, a third reader with 12 years' experience was used.

Method of Confirmation

No histology was obtained to document IMN adenopathy. All 90 patients underwent follow-up MRI at the end of chemotherapy, and 41 patients, including 10 patients with IMN adenopathy, also underwent posttreatment PET/CT. Decrease in either size or SUV (or both) of the IMNs after chemotherapy was considered confirmation of malignancy.

Statistical Analysis

Patient age and primary tumor size were summarized using median and range and compared between patients with and without IMN adenopathy using Wilcoxon rank-sum test. Features including LVI, quadrant of primary tumor, and presence or absence of axillary adenopathy were summarized in terms of percentages and compared between presence and absence of IMN adenopathy using Fisher's exact test. The McNemar test was performed to compare the prevalence of IMN adenopathy on MRI and on PET/CT.

Patient overall survival was defined as the time interval between the date of either MRI or PET, whichever was performed earlier, and the date of either last follow-up or death. Patients alive at the last follow-up were censored. Kaplan-Meier method was used to estimate overall survival at 3 years, and the log-rank test was used to compare overall survival between presence or absence of IMN adenopathy. A test with $p < 0.05$ was considered statistically significant. All statistical analyses were performed in SAS (version 9.2, SAS Institute).

Results

The 90 patients ranged in age from 25 to 72 years old (median, 44 years old). Primary tumor size ranged from 1.4 to 12.2 cm (median, 4.8 cm). Readings were concordant between the two primary readers in 85 patients and discordant in five. In three of the discordant cases, one of the two original readers called the MRI findings negative for examinations with positive PET/CT findings whereas the other two readers called the MRI findings positive as well; in one patient, one reader called findings of both examinations negative whereas the other two readers called them positive; and in the fifth discordant case, one of the readers called findings of both examinations positive whereas the other two readers considered them negative. The discordant cases were divided between the two original readers.

IMN adenopathy was identified in 14 of 90 women (16%). All 14 IMNs were seen on MRI. On PET/CT, IMNs were identified in 13 of these 14 women. The prevalence of IMN adenopathy was 16% (14/90) on MRI and 14% (13/90) on PET/CT; the difference was not statistically significant ($p = 0.317$). In seven of these 14 patients (50%), more than one IMN was detected.

Nodes detected on MRI ranged from 7 to 22 mm. Nodes on the CT portion of the PET/CT examinations measured 7–17 mm. SUV range was 1.5–16.4.

After completion of chemotherapy, IMNs were no longer identified in 12 of 14 patients (86%) including the patient with IMN adenopathy evident on MRI but not on PET/CT. These women had complete or nearly complete response in their primary tumors as well. In the two of these 14 patients (14%) who had poor responses in their primary breast tumors, IMN adenopathy improved but persisted (Fig. 2), and both patients developed metastatic disease within 6 months.

Length of follow-up for the 90 women in this study ranged from 7.2 to 59.9 months (median, 31.3 months). The median overall survival was not reached. Eleven of 90 patients (12%) were deceased by the last follow-up, including five of the 14 patients with IMN adenopathy (36%). The difference in overall survival of the two groups at 3 years (85.7% vs 53.3%) was statistically significant (log-rank test $p = 0.009$). The occurrence of IMN adenopathy was not statistically associated with size, quadrant(s) of primary tumor, presence of axillary adenopathy, or LVI in this relatively small sample size (Table 1).

Discussion

In the distant past, IMNs were removed and pathologically evaluated during extended radical mastectomies [11]. As mastectomies became less aggressive and as breast conservation became more common, IMNs were no longer routinely sampled. In the recent era of sentinel node biopsy, some surgeons again began to biopsy visible IMNs, resulting in stage migration and possible benefit owing to more aggressive medical and radiation oncology treatment [4]. However, IMNs are rarely visible, and their removal may be associated with an increase in morbidity [12].

In patients undergoing breast conservation and in patients requiring radiation after mastectomy, there is a controversy as to the risk versus benefit of including the internal mammary chain in the radiation field. Although some researchers [4, 5] have shown that radiation of IMNs (and other extraaxillary nodal groups) may improve outcome, the additional risk of radiation-induced cardiac toxicity prevents routine inclusion of this additional field. It is therefore imperative to have a reliable imaging tool to diagnose IMN adenopathy.

Routine systemic staging with PET/CT is recommended in women with clinical stage IIIA or greater breast carcinomas [13], and there are data to suggest significant upstaging in patients with stage IIB disease as well [14–16]. Multiple studies have confirmed that PET/CT is more sensitive than CT alone for the detection of IMN adenopathy [10, 17]. Eubank et al. [8] showed that PET/CT was superior to CT alone in detection of mediastinal

and IM adenopathy. In a study of 28 women with breast cancer, Bellon et al. [9] reported highly suspicious IMNs in seven women, all of whom were reported to have negative findings on chest CT. In 216 patients with clinical stage III breast cancer, Seo et al. [18] showed a positive predictive value of 87.1% for IMN metastasis on PET/CT.

Many women undergo breast MRI at diagnosis for assessment of extent of disease within the breasts. Little has been written regarding the utility of MRI for detection of IMN adenopathy. Kinoshita et al. [19] studied 43 dissected IMNs in 16 patients using a 1.5-T MR scanner with a surface coil while patients were in supine position; considering a measurement of more than 5 mm as a positive finding, they reported a 90.7% accuracy, 93.3% sensitivity, and 89.3% specificity. Zhang et al. [20] reported the presence of IMN adenopathy in 112/809 (13.8%) breast cancer patients with known nodal disease, a small fraction of which were detected by MRI. However, there were too few patients with MRI-detected IMN disease for analysis. Although benign IMNs may be seen on breast MRI, all IMNs in our series were larger than 5 mm, suggesting a higher likelihood of malignancy [19] in these women with locally advanced primary tumors.

In the present article, we have reported our experience with imaging-detected IMN adenopathy in a population of 90 women evaluated with PET/CT and breast MRI before neoadjuvant chemotherapy. Previously reported prevalence of IMN adenopathy has ranged from 9.0% to 47.5% [6, 9, 20, 21], with the highest prevalence occurring in a group undergoing extended radical mastectomy [6]. The remainder of the patients received diagnoses by imaging. Our population of women with predominantly advanced tumors (75/90 [83%] with more aggressive biology) falls within this range with a prevalence of 16%. In our study, which is the first to report the comparison between breast MRI and PET/CT for the detection of IMN adenopathy in women with breast cancer, MRI and PET/CT both identified IMNs in the same 13 women, and MRI detected a discrete additional IMN (Fig. 3) in a single additional woman.

IMN adenopathy has been reported to occur more frequently with larger primary tumors, particularly in patients with tumors in the medial breast, patients with axillary adenopathy, patients younger than 50 years old, and patients with LVI [4, 6, 7]. In this series, those findings were not confirmed, but the number of patients included in this study was underpowered to achieve statistical significance. In addition, because our entire population consisted of women with more advanced disease, nearly all patients had large tumors, many of which involved multiple quadrants, and had axillary adenopathy and LVI. This mitigated the ability to detect significant differences in these proposed predictive factors.

The presence of IMN adenopathy at presentation in women with breast cancer is associated with a poor prognosis [1–3]. This was true in our series, with a significant difference in overall survival at 3 years of 85.7% for women without IMN adenopathy compared with 53.3% for those with IMN adenopathy.

The limitations of this study include the retrospective nature of the study and the small patient population, as well as the lack of histologic confirmation of IMN adenopathy. Although FDG PET/CT is known to be quite specific in the detection of IMN metastases,

specificity of MRI for IMN adenopathy is not well studied. The patients considered to have IMN adenopathy according to our imaging criteria all had evidence of response in their IMNs that corresponded to the response in the primary tumors. Further confirmatory evidence is that, in this series, the patients deemed as having IMN adenopathy had a significantly worse prognosis than those without IMN adenopathy, which is consistent with multiple other studies comparing the outcomes in these two groups. Prospective trials (possibly with histologic confirmation) comparing breast MRI to PET/CT in women with more advanced cancers would be the ideal way to confirm our findings.

Conclusion

In women with advanced breast cancer, PET/CT is known to be valuable for detecting IMN adenopathy. Breast MRI is frequently performed before systemic staging for breast carcinoma, and this study has shown that identification of IMN adenopathy is not significantly different between MRI and PET/CT. Therefore, particular attention should be paid to the internal mammary chain when reading breast MRI examinations. Until there are more data regarding the specificity of breast MRI in the detection of IMN adenopathy, patients with possible IMN adenopathy on MRI may benefit from use of MRI and PET/CT in a complementary fashion. Evidence of IMN adenopathy on MRI or FDG PET/CT not only may alter radiation treatment plans but also provides important prognostic information.

Acknowledgments

Supported in part by National Cancer Institute core grant P30 CA008748.

We thank Jane Howard for providing the patient database.

References

1. Sugg SL, Ferguson DJ, Posner MC, Heimann R. Should internal mammary nodes be sampled in the sentinel lymph node era? Ann Surg Oncol. 2000; 7:188–192. [PubMed: 10791848]
2. Cody HS 3rd, Urban JA. Internal mammary node status: a major prognosticator in axillary node-negative breast cancer. Ann Surg Oncol. 1995; 2:32–37. [PubMed: 7834452]
3. Veronesi U, Cascinelli N, Greco M, et al. Prognosis of breast cancer patients after mastectomy and dissection of internal mammary nodes. Ann Surg. 1985; 202:702–707. [PubMed: 3000303]
4. Veronesi U, Arnone P, Veronesi P, et al. The value of radiotherapy on metastatic internal mammary nodes in breast cancer: results on a large series. Ann Oncol. 2008; 19:1553–1560. [PubMed: 18467318]
5. Stemmer SM, Rizel S, Hardan I, et al. The role of irradiation of the internal mammary lymph nodes in high-risk stage II to IIIA breast cancer patients after high-dose chemotherapy: a prospective sequential nonrandomized study. J Clin Oncol. 2003; 21:2713–2718. [PubMed: 12860949]
6. Huang O, Wang L, Shen K, et al. Breast cancer subpopulation with high risk of internal mammary lymph nodes metastasis: analysis of 2,269 Chinese breast cancer patients treated with extended radical mastectomy. Breast Cancer Res Treat. 2008; 107:379–387. [PubMed: 17457670]
7. Chen RC, Lin NU, Golshan M, Harris JR, Bellon JR. Internal mammary nodes in breast cancer: diagnosis and implications for patient management—a systematic review. J Clin Oncol. 2008; 26:4981–4989. [PubMed: 18711171]
8. Eubank WB, Mankoff DA, Takasugi J, et al. ^{18}Fluorodeoxyglucose positron emission tomography to detect mediastinal or internal mammary metastases in breast cancer. J Clin Oncol. 2001; 19:3516–3523. [PubMed: 11481358]

9. Bellon JR, Livingston RB, Eubank WB, et al. Evaluation of the internal mammary lymph nodes by FDG-PET in locally advanced breast cancer (LABC). Am J Clin Oncol. 2004; 27:407–410. [PubMed: 15289736]
10. Cermik TF, Mavi A, Basu S, Alavi A. Impact of FDG PET on the preoperative staging of newly diagnosed breast cancer. Eur J Nucl Med Mol Imaging. 2008; 35:475–483. [PubMed: 17957366]
11. Urban JA. Radical excision of the chest wall for mammary cancer. Cancer. 1951; 4:1263–1285. [PubMed: 14886886]
12. Sacchini G, Borgen PI, Galimberti V, et al. Surgical approach to internal mammary lymph node biopsy. J Am Coll Surg. 2001; 193:709–713. [PubMed: 11768690]
13. National Comprehensive Cancer Network (NCCN) website. [Accessed June 5, 2015] NCCN clinical practice guidelines in oncology (NCCN Guidelines): breast cancer screening and diagnosis, version 1.2012. NCCN.org. Updated July 16, 2012
14. Groheux D, Hindie E, Delord M, et al. Prognostic impact of ^{18}FDG-PET-CT findings in clinical stage III and IIB breast cancer. J Natl Cancer Inst. 2012; 104:1879–1887. [PubMed: 23243198]
15. Aukema TS, Straver ME, Peeters MJ, et al. Detection of extra-axillary lymph node involvement with FDG PET/CT in patients with stage II-III breast cancer. Eur J Cancer. 2010; 46:3205–3210. [PubMed: 20719497]
16. Koolen BB, Vrancken Peeters MJ, Aukema TS, et al. ^{18}F-FDG PET/CT as a staging procedure in primary stage II and III breast cancer: comparison with conventional imaging techniques. Breast Cancer Res Treat. 2012; 131:117–126. [PubMed: 21935602]
17. Danforth DN Jr, Aloj L, Carrasquillo JA, et al. The role of ^{18}F-FDG-PET in the local/regional evaluation of women with breast cancer. Breast Cancer Res Treat. 2002; 75:135–146. [PubMed: 12243506]
18. Seo MJ, Lee JJ, Kim HO, et al. Detection of internal mammary lymph node metastasis with ^{18}F-fluorodeoxyglucose positron emission tomography/computed tomography in patients with stage III breast cancer. Eur J Nucl Med Mol Imaging. 2014; 41:438–445. [PubMed: 24196918]
19. Kinoshita T, Odagiri K, Andoh K, et al. Evaluation of small internal mammary lymph node metastases in breast cancer by MRI. Radiat Med. 1999; 17:189–193. [PubMed: 10440106]
20. Zhang YJ, Oh JL, Whitman GJ, et al. Clinically apparent internal mammary nodal metastasis in patients with advanced breast cancer: incidence and local control. Int J Radiat Oncol Biol Phys. 2010; 77:1113–1119. [PubMed: 20004535]
21. Wang CL, Eissa MJ, Rogers JV, Aravkin AY, Porter BA, Beatty JD. ^{18}F-FDG PET/CT–positive internal mammary lymph nodes: pathologic correlation by ultrasound-guided fine-needle aspiration and assessment of associated risk factors. AJR. 2013; 200:1138–1144. [PubMed: 23617501]

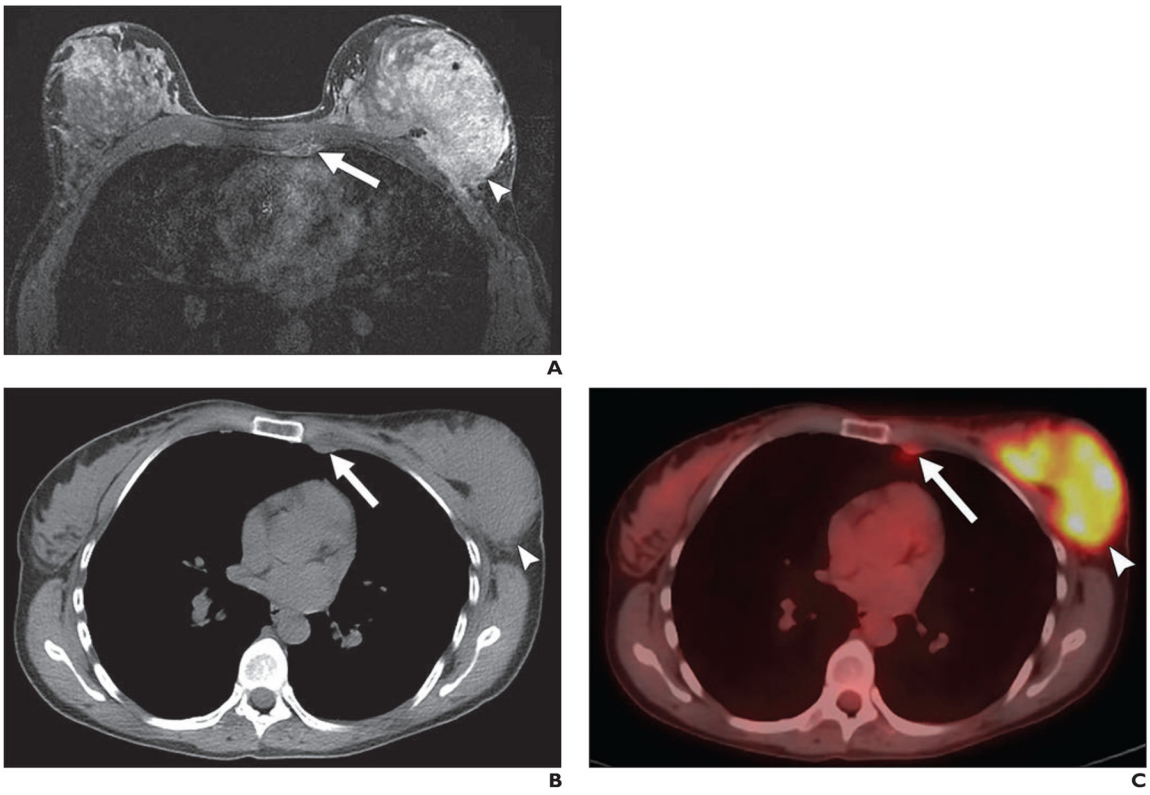

Fig. 1.

Left breast cancer of left internal mammary node adenopathy in 36-year-old woman with poorly differentiated invasive ductal carcinoma. Pretreatment imaging included both MRI and PET/CT examinations.

A, T1-weighted axial contrast-enhanced breast MR image shows tumor infiltration of entire left breast (*arrowhead*) and enlarged left internal mammary node (*arrow*).

B, Axial unenhanced chest CT image shows left breast cancer (*arrowhead*) and enlarged left internal mammary node (*arrow*).

C, Axial fused PET/CT image shows hypermetabolic activity within left breast cancer (*arrowhead*) and left internal mammary node (*arrow*) consistent with metastatic disease to node.

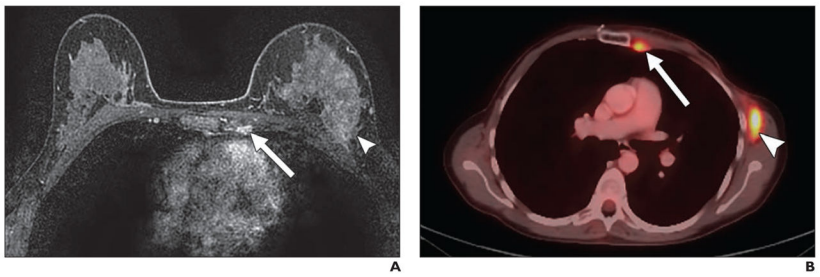

Fig. 2.

Posttreatment imaging of same patient as Fig. 1.

A, Axial MR image after neoadjuvant chemotherapy shows decreased extent of tumor (*arrowhead*) in left breast with persistently enlarged internal mammary node (*arrow*).

B, Axial fused PET/CT image 6 months after left mastectomy shows recurrent left chest wall tumor (*arrowhead*) and persistent left internal mammary adenopathy (*arrow*).

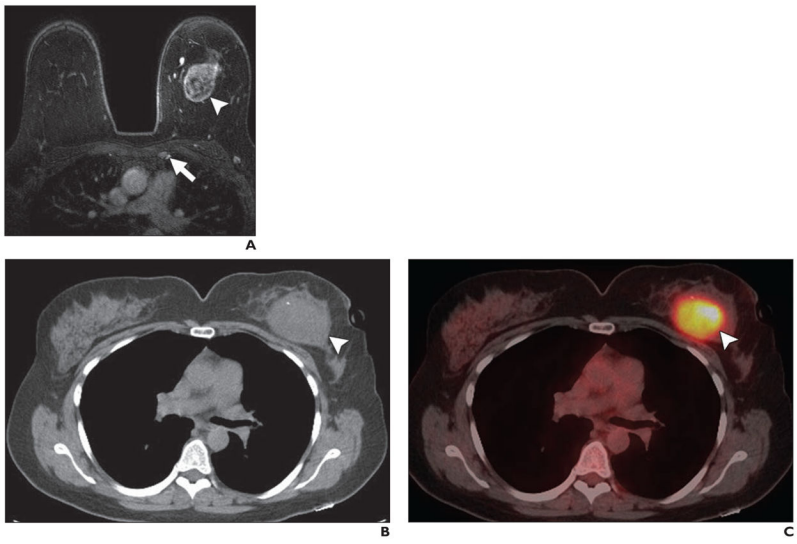

Fig. 3.

Left breast cancer with adenopathy of left internal mammary node in 42-year-old woman with highgrade infiltrating ductal carcinoma with necrosis. Pretreatment imaging included both MRI and PET/CT examinations, and adenopathy was evident on MRI but not on PET/CT.

A, T1-weighted axial contrast-enhanced breast MR images shows necrotic left breast mass (*arrowhead*) and 0.8-cm left internal mammary node (*arrow*).

B, Axial unenhanced chest CT image shows left breast cancer (*arrowhead*), but adenopathy of internal mammary node is not evident.

C, Axial fused PET/CT image at same level shows hypermetabolic left breast cancer (*arrowhead*), but hypermetabolic activity within internal mammary node is not evident.

TABLE 1

Patient Characteristics by Presence or Absence of Internal Mammary Node (IMN) Adenopathy on PET/CT and MRI

Parameter	IMN Adenopathy on PET/CT?			IMN Adenopathy on MRI?		
	No (*n* = 77)	Yes (*n* = 13)	*p*	No (*n* = 76)	Yes (*n* = 14)	*p*
Age (y), median (range)	46 (25–72)	41 (32–67)	0.231	46 (25–72)	41 (32–67)	0.209
Primary tumor size (cm), median (range)	4.3 (1.4–12.2)	6.5 (2.7–9.0)	0.126	4.3 (1.4–12.2)	6.5 (2.7–9.0)	0.09
Quadrant(s) affected			0.068			0.228
Central	17 (22)	0		16 (21)	1 (7)	
Inner	9 (12)	1 (8)		9 (12)	1 (7)	
Outer	21 (28)	2 (15)		21 (28)	2 (14)	
Multicentric	30 (39)	10 (77)		30 (40)	10 (71)	
Axillary adenopathy			0.285			0.507
Absent	20 (26)	1 (8)		19 (25)	2 (14)	
Present	57 (74)	12 (92)		57 (75)	12 (86)	
Lymphovascular invasion			0.364			0.478
Not evident	60 (78)	9 (69)		59 (78)	10 (71)	
Evident	15 (19)	3 (23)		15 (20)	3 (21)	
Suspicious	2 (3)	1 (8)		2 (3)	1 (7)	

Note—Except where otherwise indicated, data are no. with percentages in parentheses.